Article
JOURNAL OF UNIVERSITY OF BABYLON
For Pure and Applied Sciences (JUBPAS)
Vol.33 ; No.2 | 2025

Influence of the psd-shell Model with He^4 Core and Hartree-Fock Calculations on the Nuclear Structure of Ne^{20}

Ari Karim Ahmed *
*Department of Physics, College of Education, University of Sulaimani,
ari.ahmed@univsul.edu.iq 46001, Sulaimania, Iraq

تأثير نموذج القشرة psd مع قلب He^4 وحسابات هارترى-فوك على التركيب النووي لـNe^{20}

ئارى كريم أحمد*[1]

القسم الفيزياء، الكلية التربية، الجامعة السليمانية، ari.ahmed@univsul.edu.iq، صندوق بريد 46001، السليمانية، العراق

Accepted: 18/4/2025 **Published:** 30/6/2025

ABSTRACT

Background:
A detailed study of the nuclear structure of Ne^{20} has been conducted using the nuclear shell model in conjunction with Hartree-Fock parameterization techniques to provide a deeper understanding of its structural properties.
Materials and Methods:
The investigation utilized the psd model space along with the PSDMK effective interaction, taking He^4 as an inert core. The model treats the remaining 16 nucleons as active particles interacting within the defined space. Radial wave functions essential for calculating matrix elements were generated using the Hartree-Fock method with various Skyrme force parameterizations, including SkXcsb, SkXta, and SLy4. In addition, harmonic oscillator (HO) wave functions were employed for comparative analysis to evaluate the effect of different single-particle bases on nuclear observables.
Results:
Several nuclear properties were systematically analyzed, such as longitudinal electron scattering form factors, low-lying energy levels, B(E2) transition strengths, magnetic dipole moments, electric quadrupole moments, root mean square charge radii, and total binding energy.
Conclusions:
This study emphasizes the benefits of utilizing a He^4 core in shell-model calculations for Ne^{20} by modeling it as a system of five alpha-like clusters. The results indicate that such a cluster-based approach improves theoretical predictions and offers a robust framework for exploring nuclear structure phenomena in light nuclei.
Keywords:

Shell Model; Hartree-Fock; Nuclear Structure; psd-model space; He^4core; Ne^{20}.

ISSN: 2312-8135 | Print ISSN: 1992-0652
info@journalofbabylon.com | jub@itnet.uobabylon.edu.iq | www.journalofbabylon.com

ISSN: 2312-8135 | Print ISSN: 1992-0652
info@journalofbabylon.com | jub@itnet.uobabylon.edu.iq | www.journalofbabylon.com

INTRODUCTION

Electron scattering is a critical tool for investigating nuclear structure via electromagnetic interaction of electrons with the nucleus, serving as a key source of experimental data for theoretical models. It is efficiency comes from the well-understood electromagnetic interaction, accurately described by quantum electrodynamics, and the relative weakness of this interaction. Omar A. et al. investigated the nuclear structure of positive parity states of $Ne^{20,22}$ using the sd-model space as O^{16}-core [1]. The inelastic longitudinal scattering form factor C2 for Ne^{20} was investigated [2], incorporating core polarization effects and the Tassie model. One study focused on the C2 form factor for Ne^{20} are calculated using the $sdpf$-shell model space includes core-polarization effect. In the work Ne^{20} is a O^{16}-core with four nucleons outside the Corey filling over the $1d_{5/2}, 2s_{1/2}$ $1d_{3/2}, 2p_{1/2}, 2p_{3/2}$, $1f_{7/2}$, and $1f_{5/2}$ shell space [3]. In another study, various density profiles were analyzed to explore the ground-state structure of Ne^{20} using the antisymmetrized quasicluster model [4]. The present study examines the Ne^{20} nucleus by employing the psd-model space to analyze its energy spectra, reduced transition probabilities, magnetic dipole moments, nuclear root-mean-square radii, binding energy, and longitudinal inelastic electron scattering form factors [5]. The psd-model space includes active shells $1p_{1/2}, 1p_{3/2}, 1d_{3/2}, 1d_{5/2}$, and $2s_{1/2}$ above the inert He^4 nucleus core, where the $(1s)^4$ configuration remains closed. This model space features center-of-mass motion and employs psd-model space interactions, such as PSDMK and PSDMWK, to connect the p- and sd-model spaces [5]. The PSDMK interaction comes from the pw-interaction inside the sd-model space [6]. It contains the active $1d_{5/2}$, $2s_{1/2}$, and $1d_{3/2}$ orbitals atop an inert O^{16} core. Furthermore, the p-model space, with the $CKPOT$ interaction, involves the $1p_{1/2}$, and $1p_{3/2}$ orbitals above the inert He^4 core [7].

THEORETICAL BACKGROUND

The many-particle, nucleus, reduced matrix element in spin space of the electron scattering between the initial and final states, $\langle J_i||\hat{T}^{\eta}_{J,t_z}(q)||J_f\rangle$, for model space is given as the sum of the one-body density matrix element (OBDM) times the single-particle matrix elements of the electron scattering, $\langle J_i||\hat{T}^{\eta}_{J,t_z}(q)||J_f\rangle$, or

$$\langle J_i||\hat{T}^{\eta}_{J,t_z}(q)||J_f\rangle = \sum_{j_i,j_f} OBDM_{J,t_z}(J_i,J_f)\,\langle J_i||\hat{T}^{\eta}_{J,t_z}(q)||J_f\rangle \qquad (1)$$

Where J_i and J_f label initial and final nuclear states respectively and j_i and j_f label single-particle states for the shell model space. The symbol $\hat{T}^{\eta}$ is nuclear spins anyone of $\hat{T}^{Coulmb}$, $\hat{T}^{electric}$, or $\hat{T}^{magnetic}$ and $t_z = 1/2$ for a proton and $t_z = -1/2$ for a neutron

The electron scattering form factor has a longitudinal $F_L(q)$ and a transverse component, $F_T(q)$ and can be written in terms of reduced matrix elements of the electromagnetic transition operators of electron scattering, including the finite-size and center of mass correction form factors [8, 9]

ISSN: 2312-8135 | Print ISSN: 1992-0652 | jub@itnet.uobabylon.edu.iq | www.journalofbabylon.com | info@journalofbabylon.com

$$|F_\eta^J(q)|^2 = \frac{4\pi}{Z^2(2J_i+1)} |\sum_{t_z} e(t_z) \left\langle J_f \left| \left| \hat{T}^\eta_{J,t_z}(q) \right| \right| J_i \right\rangle|^2 \times |F_{cm}(q)|^2 |F_{fs}(q)|^2 \quad (2)$$

Where $F_\eta = F_{C,E,M}$ that is represents each of Coulomb, transverse electric and magnetic form factors. Since $Z\alpha \ll 1$, they are given in plane-wave first order Born approximation for nuclear transitions from initial state of angular momentum to final state [10, 11], with using Wigner-Eckart theorem [10] the total longitudinal (L)and transverse (T)form factors are given by

$$|F_L(q)|^2 = \frac{1}{2J_i+1} \sum_{J\geq 0} |\langle J_f || \hat{T}^{Coulomb}_{J,t_z}(q) || J_i \rangle|^2 \quad (3)$$

$$|F_T(q)|^2 = \frac{1}{2J_i+1} \sum_{J\geq 1} \{ |\langle J_f || \hat{T}^{electric}_{J,t_z}(q) || J_i \rangle|^2 + |\langle J_f || \hat{T}^{magnetic}_{J,t_z}(q) || J_i \rangle|^2 \} \quad (4)$$

The total form factor can be expressed from the sum of its components [12]

$$|F(q,\theta)|^2 = (1 - \omega^2/q^2)|F_L(q)|^2 + \left[\frac{1}{2}(1 - \omega^2/q^2) + tan^2\frac{\theta}{2}\right]|F_L(q)|^2 \quad (5)$$

where θ is the electron scattering angle.

The Skyrme potential is employed as the central potential, characterized by its role as a mean-field potential. This potential approximates the collective effect of all nucleons within the nucleus, simulating the interactions among them while representing the realistic forces between nucleon pairs and triplets. Mathematically, the Skyrme interaction, V_{Skyrme}, is expressed as a combination of two-body and three-body components [13].

$$\hat{V}_{Skyrme} = \sum_{i<j} V^{(2)}_{ij} + \sum_{i<j<k} V^{(3)}_{ijk} \quad (6)$$

The two-body part interaction also contains the mean central, spin-orbit, and the tensor parts. In momentum space it can be written as [14].

$$\hat{V}_{Skyrme}(\boldsymbol{r}_1, \boldsymbol{r}_2) = \hat{V}^m + \hat{V}^{L.S} + \hat{V}^t \quad (7)$$

Where

$$\hat{V}^m = t_0\left(1 + x_0\hat{P}_\sigma\right)\delta_{12} + \frac{t_1}{2}\left(1 + x_1\hat{P}_\sigma\right)\left(\hat{\boldsymbol{k}}_1^2 + \hat{\boldsymbol{k}}_2^2\right)\delta_{12} + t_2(1 + x_2\hat{P}_\sigma)\hat{\boldsymbol{k}}_2.\hat{\boldsymbol{k}}_1\delta_{12} + \frac{t_3}{6}(1 + x_3\hat{P}_\sigma)\rho^\alpha(\boldsymbol{r})\delta_{12} \quad (8)$$

$$\hat{V}^{L.S} = it_4 + (\hat{\sigma}_1 + \hat{\sigma}_2).\hat{\boldsymbol{k}}_2 \times \hat{\boldsymbol{k}}_1\delta_{12} \quad (9)$$

$$\hat{V}^t = \frac{t_e}{2}\left\{\left[3(\hat{\sigma}_1.\hat{\boldsymbol{k}}_2)(\hat{\sigma}_2.\hat{\boldsymbol{k}}_2) - (\hat{\sigma}_1.\hat{\sigma}_2)\hat{\boldsymbol{k}}_2^2\right]\delta_{12} + \left[3(\hat{\sigma}_1.\hat{\boldsymbol{k}}_1)(\hat{\sigma}_2.\hat{\boldsymbol{k}}_1) - (\hat{\sigma}_1.\hat{\sigma}_2)\hat{\boldsymbol{k}}_1^2\right]\delta_{12}\right\} + t_s\left[3(\hat{\sigma}_1.\hat{\boldsymbol{k}}_2)(\hat{\sigma}_2.\hat{\boldsymbol{k}}_1) - (\hat{\sigma}_1.\hat{\sigma}_2)\hat{\boldsymbol{k}}_2.\hat{\boldsymbol{k}}_1^2\right]\delta_{12} \quad (10)$$

δ_{12} is the Dirac delta function, $\delta_{12} = \delta(\boldsymbol{r}_1 - \boldsymbol{r}_2)$, $\hat{\sigma}_1$ and $\hat{\sigma}_2$ are the vector of Pauli spin matrices for the first and second nucleon respectively, and three body part can be written as

$$V^{(3)}_{Skyrme} = t_3\delta_{12}\delta_{13} \quad (11)$$

ISSN: 2312-8135 | Print ISSN: 1992-0652
info@journalofbabylon.com | jub@itnet.uobabylon.edu.iq | www.journalofbabylon.com

The $\hat{\boldsymbol{k}}_1$ and $\hat{\boldsymbol{k}}_2$ operators are the relative momentums, wave vectors, of the first and second nucleon which operate on the wave functions to the right $|\psi\rangle$ and to the left $\langle\psi|$ respectively and having the form

$$\hat{\boldsymbol{k}}_1 = \frac{1}{2i}\left(\vec{\nabla}_1 - \vec{\nabla}_2\right), \ \hat{\boldsymbol{k}}_2 = -\frac{1}{2i}\left(\overleftarrow{\nabla}_1 - \overleftarrow{\nabla}_2\right) \quad (12)$$

The reduced transition probability [12], representing the probability of a nuclear transition between states, is mathematically expressed as:

$$B(\eta J) = \frac{Z^2}{4\pi}\left[\frac{(2J+1)!!}{k^J}\right]^2 |F_J^{\eta}(k)|^2 \quad (13)$$

Where $k = \frac{E_x}{\hbar c}$

RESULTS AND DISCUSSION

Utilizing the PSDMK interaction with the NushellX code with parallel advanced computer and the psd-model space, one-body density matrix elements (OBDM) were generated in the current investigation [12]. The radial wave functions of the single-particle matrix elements were calculated using the Skyrme interaction, from which a one-body potential in HF theory with SkXcsb, SkXta, and SLy4 parameterizations could be produced, as well as a harmonic oscillator (HO) potential. The SLy4 potential, along with the psd-model space, indicates that the root mean square (rms) charge radius is 2.955 fm, which is consistent with the experimental value of 3.005 fm [15], while the calculated binding energy is 152.088 MeV, which is in reasonable agreement with the experimental value of 160.64 MeV [16]. The elastic Coulomb $C0$ form factors for the ground state of the Ne^{20} nucleus ($0^+, 0\ MeV$) were computed using wave function from the psdmodel space, along with parameterizations from $Skxcsb, Skxta,$ and $Sly4$ and harmonic oscillator (HO) potential. The results, depicted in Figure 1, are compared against experimental data from Ref. [17]. Every potential type is in the best agreement for every momentum transfer region, particularly for SLy4 parameterization.

ISSN: 2312-8135 | Print ISSN: 1992-0652
info@journalofbabylon.com | jub@itnet.uobabylon.edu.iq | www.journalofbabylon.com

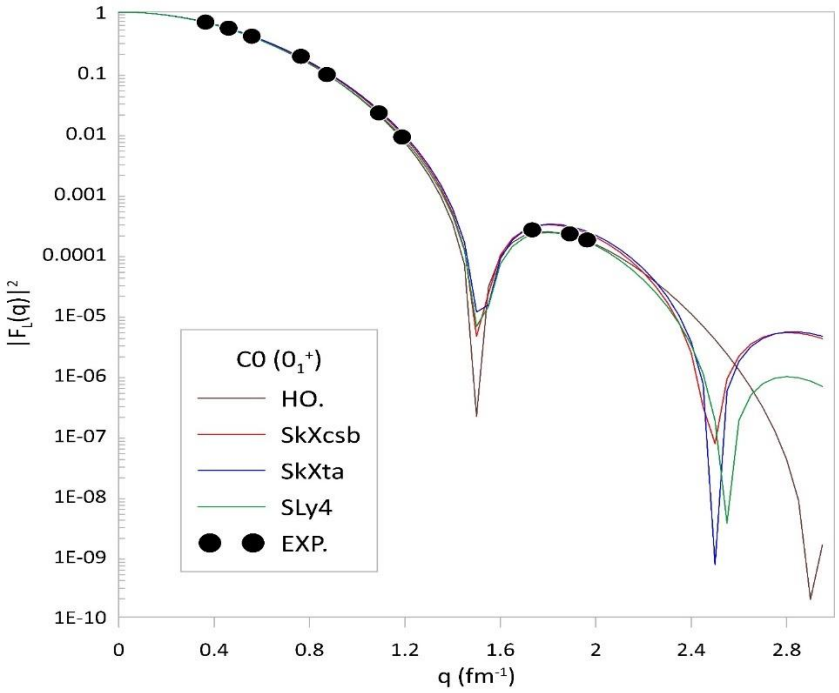

Figure (1): Longitudinal C0 form factor for $(0^+, 0\,MeV)$ of Ne^{20} compared with the experimental value [17].

The inelastic longitudinal C2 form factors for the 2_1^+ (1.633 MeV) and 2_2^+(7.422 MeV) states are presented in Figure 2. Across all momentum transfer values, the 2_1^+ state shows good agreement with all potential types, with the SLy4 parameterization exhibiting an excellent fit to the experimental data [17]. However, at $q = 1.73333\,fm^{-1}$, the results align more closely with the harmonic oscillator (HO) potential. For the 2_2^+ state, the form factors qualitatively match the experimental data within the range $q = 0.58\,to\,1.28\,fm^{-1}$, while for $q = 1.36\,to\,1.8\,fm^{-1}$, they achieve both qualitative and quantitative agreement, particularly with the SLy4 parameterization, which most accurately reproduces the experimental results.

ISSN: 2312-8135 | Print ISSN: 1992-0652
info@journalofbabylon.com | jub@itnet.uobabylon.edu.iq | www.journalofbabylon.com

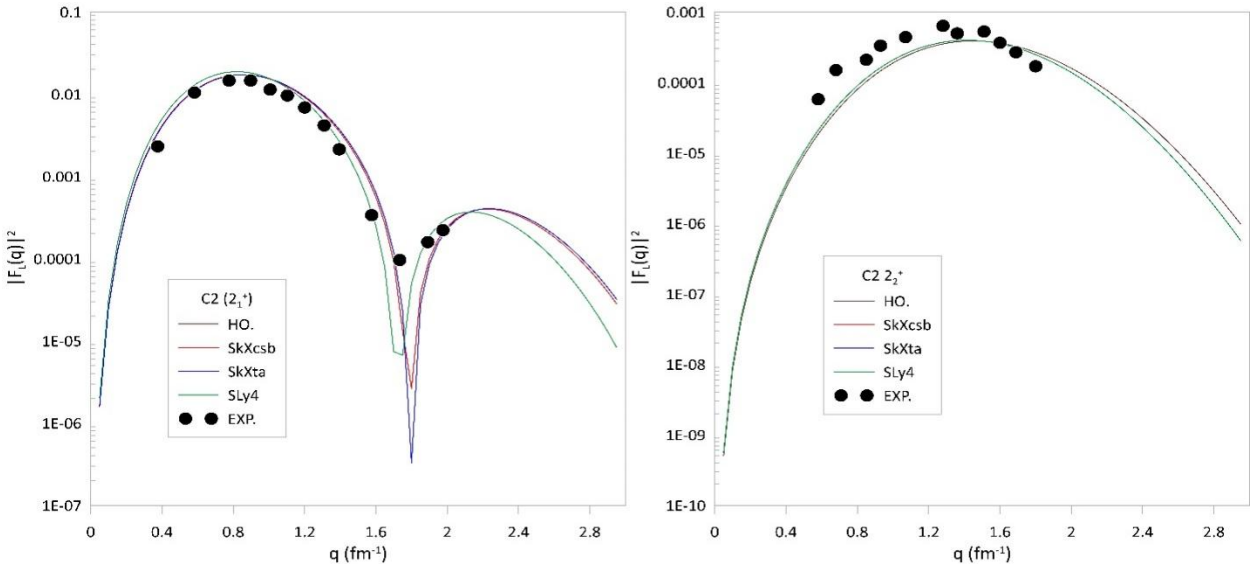

Figure (2): Longitudinal C2 form factor for the 2_1^+ (1.633 MeV) and 2_2^+(7.422 MeV) of Ne^{20} compared with the experimental value [17].

The inelastic longitudinal C2 form factor for the 2_3^+ (7.833 MeV) is presented in Figure 3. It exhibits a strong agreement only at $q = 0.59\, fm^{-1}$. However, within the range $q = 0.6\ to\ 1.36\, fm^{-1}$, the form factor qualitatively aligns well with the experimental data [17]. In contrast, for $q = 1.52\ to\ 1.36\, fm^{-1}$, the agreement worsens, resulting in a poorer fit due to the 2_3^+ state exhibiting rotational behavior.

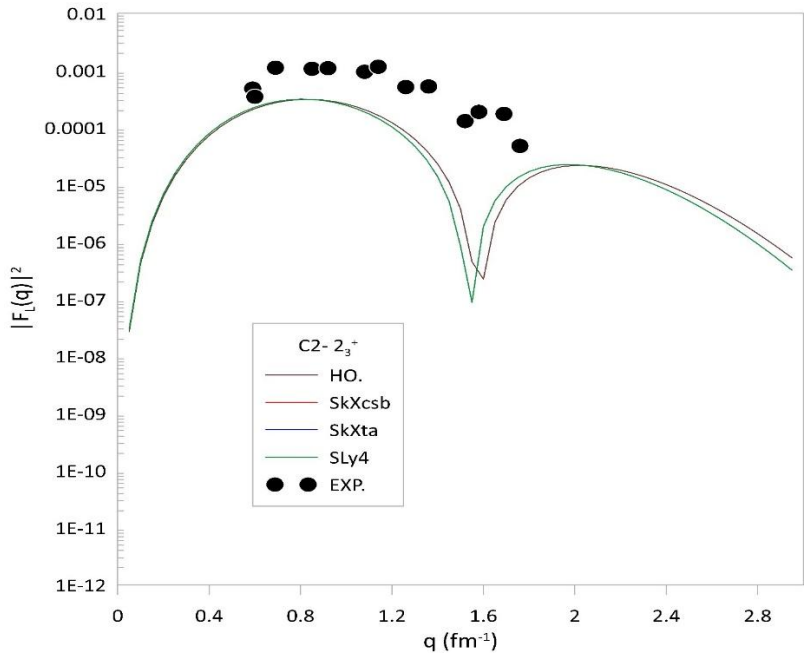

Figure (3): Longitudinal C2 form factor for the 2_3^+ (7.833 MeV) of Ne^{20} compared with the experimental value [17].

ISSN: 2312-8135 | Print ISSN: 1992-0652
info@journalofbabylon.com | jub@itnet.uobabylon.edu.iq | www.journalofbabylon.com

The longitudinal C4 form factor for the 4_1^+ (4.2477MeV) of Ne^{20} is illustrated in Figure 4. All parameterizations, as well as the harmonic oscillator (HO) potential, show excellent agreement with the experimental data [17] in the range $q = 0.9\ to\ 1.38138\ fm^{-1}$. However, the SLy4 parameterization provides the best fit within the range $q = 1.56\ to\ 2\ fm^{-1}$, outperforming the other potentials.

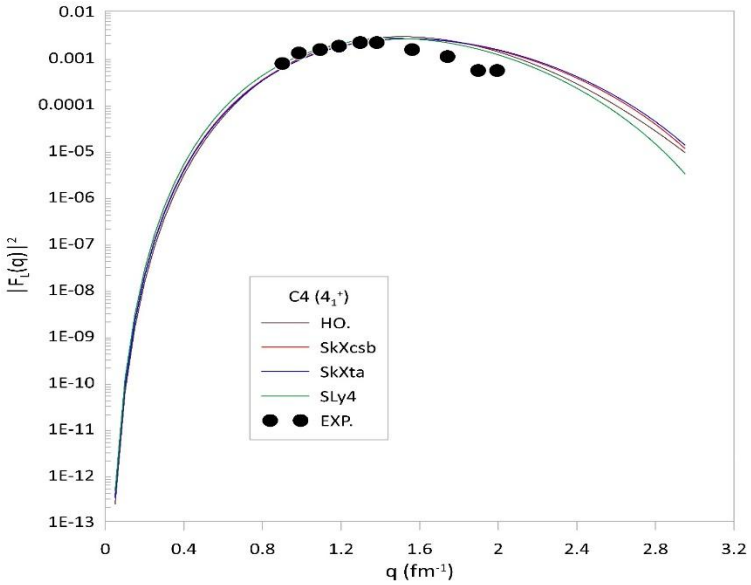

Figure (4): Longitudinal C4 form factor for the 4_1^+ (4.2477MeV) of Ne^{20} compared with the experimental value [17].

Furthermore, the energy levels of low-lying positive parity states in Ne^{20} have been determined using the psd -model space with the PSDMK interaction. Figure 5 presents a comparison between the calculated energy levels and the experimental energy spectrum [12]. The theoretical results accurately reproduce the experimental values for the 0_1^+, 2_1^+, and 4_1^+ states, while the shell model calculations with the $SkXcsb$ parameterization effectively capture the dense structure of positive parity states. Additionally, most of the other states are in good agreement with experimental data; however, the 3_1^+ , and 4_2^+ states are overestimated, yielding higher energy values than observed experimentally. The overall comparison demonstrates that the PSDMK interaction successfully reproduces the general structure of the energy spectrum, particularly for low-lying states. Nevertheless, discrepancies in the higher excitation regions, especially in the placement of the 3_1^+ , and 4_2^+ levels, suggest that further refinements in the interaction parameters may enhance predictive accuracy.

ISSN: 2312-8135 | Print ISSN: 1992-0652
info@journalofbabylon.com | jub@itnet.uobabylon.edu.iq | www.journalofbabylon.com

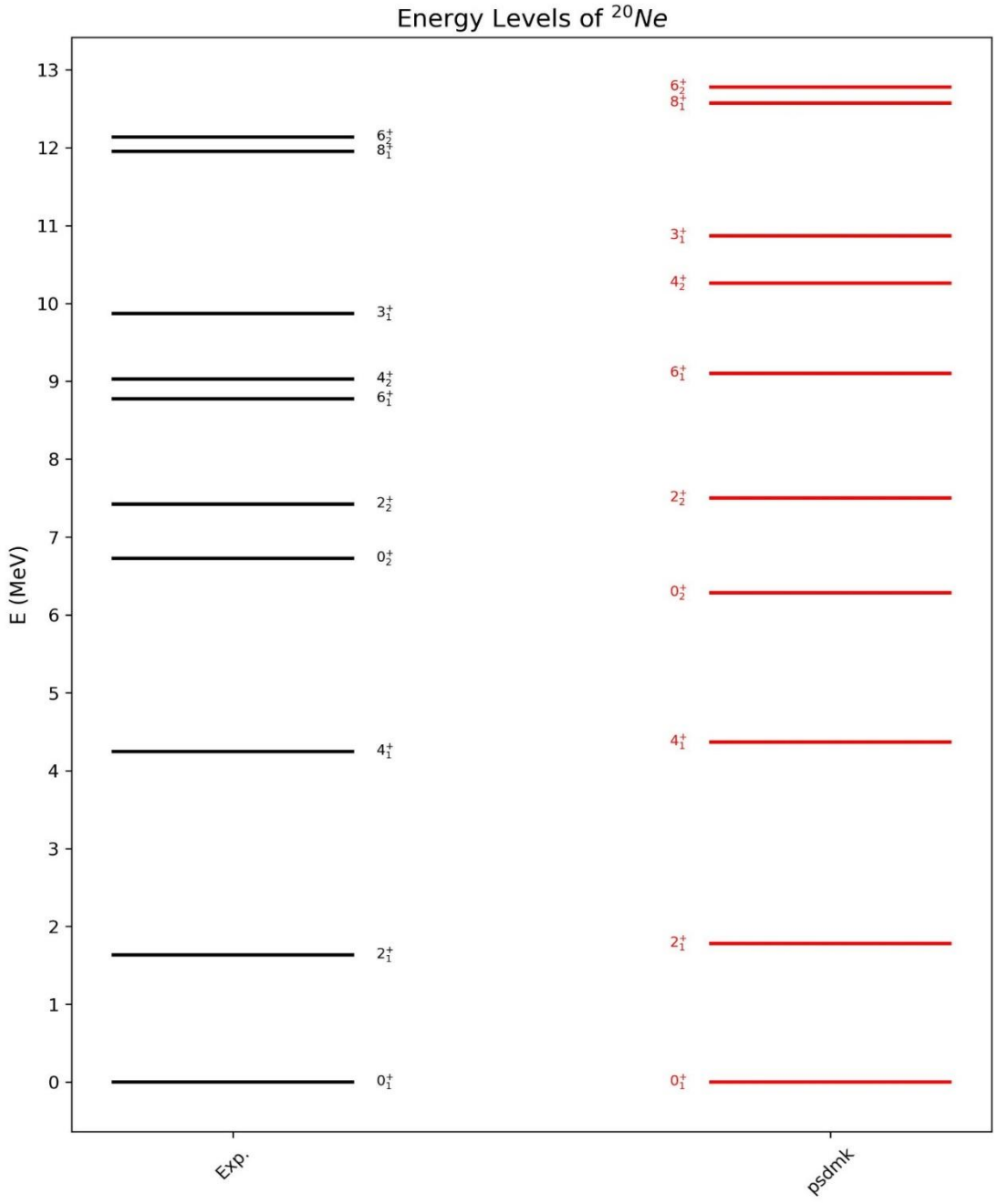

Figure (5): Energy levels of the positive parity states of the Ne^{20} nucleus, compared with experimental data [12].

In current work, calculations were performed for reduced transition probabilities $B(\eta J)$, magnetic dipole moments (μ), and electric quadrupole moments (Q). The electric quadrupole $B(E2)$ transition probabilities among low-lying nuclear states were determined using standard effective charges of $\delta e_p = 0.5$ and $\delta e_n = 0.5$. The calculated reduced transition probabilities, presented in Table 1, exhibit excellent agreement with experimental data [18]. Furthermore, the

ISSN: 2312-8135 | Print ISSN: 1992-0652
info@journalofbabylon.com | jub@itnet.uobabylon.edu.iq | www.journalofbabylon.com

results obtained using the psd-model space provide a more accurate description of nuclear transitions compared to those derived from the sd-model space, as reported in Ref. [1].

Table 1. Reduced transition probabilities of positive parity states of Ne^{20} compared with experimental [18].

J^{π}	$B(\eta J)\ e^2fm^{2J}$		
	wL	$Exp.$	$psdmk$
2_1^+	E2	340(30)	370
2_2^+	E2	0.13(0.03)	0.1281
2_3^+	E2	0.83(0.13)	1.870
4_1^+	E4	-	0.4241E+05
4_2^+	E4	-	0.1313E+04

Conversely, the magnetic dipole moment and electric quadrupole moment, calculated using specific effective charge values for the model space, are presented in Table 2. The obtained results demonstrate a strong agreement with the experimental data [19], further validating the reliability of the applied theoretical framework.

Table 2. Magnetic dipole and electric quadrupole moments of Ne^{20} compared with experimental [19]

PSDMK	e_p	e_n	g_{lp}	g_{ln}	g_{sp}	g_{sn}	g_{tp}	g_{tn}
	1.5	0.5	1	0	5.586	-3.826	0	0
	μ nm				$Q\ b$			
State	$psdmk$		$EXP.$		$psdmk$		$EXP.$	
2_1^+	1.016		1.08(8)		-0.1567		-0.23(3)	
4_1^+	2.038		1.7(14)		-0.1996			
2_2^+	1.086				0.0901			
2_3^+	1.047				-0.0960			
4_2^+	2.142				-0.1015			
2_4^+	1.267				0.0910			
3_1^+	1.797				-0.0439			
1_1^+	0.555				0.0309			

ISSN: 2312-8135 | Print ISSN: 1992-0652
info@journalofbabylon.com | jub@itnet.uobabylon.edu.iq | www.journalofbabylon.com

CONCLUSION

Utilizing the psd-model space with a ^4He core and the PSDMK interaction, this study examined the nuclear structure of ^{20}Ne. Calculations of energy spectra, transition probabilities, and form factors—especially with SLy4—show strong agreement with experimental data. The results affirm the reliability of the psd space and highlight clustering effects via ^4He cores. This approach enhances predictive power and supports further developments in nuclear structure modeling.

Conflict of interests:

There are non-conflicts of interest.

References

[1] O. A. Alswaidawi and A. Alzubadi, "Electroexcitation Form Factors and Deformation of 20,22Ne Isotopes Based on the Shell Model and Hartree-Fock plus BCS Calculations." *East European Journal of Physics*, no. 2, pp. 138-149, 2023, doi: 10.26565/2312-4334-2023-2-13.

[2] A. K. Hamoudi, R. Radhi, F. I. Shrrad Al-Taie, and R. Mohammed, "CALCULATION OF THE INELASTIC LONGITUDINAL ELECTRON SCATTERING OF 20Ne AND 24Mg NUCLEI." *Journal of Wasit for Science and Medicine*, vol. 2, no. 1, pp. 39-52, 2022, doi: 10.31185/jwsm.26.

[3] J. Khalid S., " Longitudinal form factor for some sd-shell nuclei using large scale model space." *International Journal of Science and Technology*, vol. 1, no. 3, pp. 140-143, Sep. 2011.

[4] Y. Yamaguchi, W. Horiuchi, and N. Itagaki, "Evidence of bicluster structure in the ground state of Ne20." *Physical Review C*, vol. 108, no. 1, 2023, doi: 10.1103/physrevc.108.014322.

[5] Y. Utsuno and S. Chiba, "Multiparticle-multihole states aroundO16and correlation-energy effect on the shell gap." *Physical Review C*, vol. 83, no. 2, 2011, doi: 10.1103/physrevc.83.021301.

[6] B. M. Preedom and B. H. Wildenthal, "Shell-Model Calculations forNa22andNe22." *Physical Review C*, vol. 6, no. 5, pp. 1633-1644, 1972, doi: 10.1103/physrevc.6.1633.

[7] S. Cohen and D. Kurath, "Effective interactions for the 1p shell." *Nuclear Physics*, vol. 73, no. 1, pp. 1-24, 1965, doi: 10.1016/0029-5582(65)90148-3.

[8] R. Hofstadter, "Electron Scattering and Nuclear Structure." *Reviews of Modern Physics*, vol. 28, no. 3, pp. 214-254, 1956, doi: 10.1103/revmodphys.28.214.

[9] "Centre-of-mass effects in the nuclear shell-model." *Proceedings of the Royal Society of London. Series A. Mathematical and Physical Sciences*, vol. 232, no. 1191, pp. 561-566, 1955, doi: 10.1098/rspa.1955.0239.

[10] H. Euteneuer, "Elastic electron scattering from the multipole moment distributions ofMg25." *Physical Review C*, vol. 16, no. 5, pp. 1703-1711, 1977, doi: 10.1103/physrevc.16.1703.

[11] T. W. Donnelly and J. D. Walecka, "Electron Scattering and Nuclear Structure." *Annual Review of Nuclear Science*, vol. 25, no. 1, pp. 329-405, 1975, doi: 10.1146/annurev.ns.25.120175.001553.

[12] B. Brown and W. Rae, "The Shell-Model Code NuShellX@MSU." *Nuclear Data Sheets*, vol. 120, pp. 115-118, 2014, doi: 10.1016/j.nds.2014.07.022.

[13] E. K. Warburton and B. A. Brown, "Effective interactions for the 0*p*1*s*0*d*nuclear shell-model space." *Physical Review C*, vol. 46, no. 3, pp. 923-944, 1992, doi: 10.1103/physrevc.46.923.

[14] D. Vautherin, "Hartree-Fock Calculations with Skyrme." *Physical Review C*, vol. 7, no. 1, pp. 296-316, 1973, doi: 10.1103/physrevc.7.296.

[15] I. Angeli and K. Marinova, "Table of experimental nuclear ground state charge radii: An update." *Atomic Data and Nuclear Data Tables*, vol. 99, no. 1, pp. 69-95, 2013, doi: 10.1016/j.adt.2011.12.006.

[16] D. Tilley, C. Cheves, J. Kelley, S. Raman, and H. Weller, "Energy levels of light nuclei, A = 20." *Nuclear Physics A*, vol. 636, no. 3, pp. 249-364, 1998, doi: 10.1016/s0375-9474(98)00129-8.

[17] S. Mitsunobu and Y. Torizuka, "Form Factors of the Monopole Transitions inNe20by Inelastic Electron Scattering." *Physical Review Letters*, vol. 28, no. 14, pp. 920-922, 1972, doi: 10.1103/physrevlett.28.920.

[18] B. Pritychenko, M. Birch, B. Singh, and M. Horoi, "Tables of E2 transition probabilities from the first 2+ states in even–even nuclei." *Atomic Data and Nuclear Data Tables*, vol. 107, pp. 1-139, 2016, doi: 10.1016/j.adt.2015.10.001.

[19] N. Stone, "Table of nuclear electric quadrupole moments." *Atomic Data and Nuclear Data Tables*, vol. 111, pp. 1-28, 2016, doi: 10.1016/j.adt.2015.12.002.

ISSN: 2312-8135 | Print ISSN: 1992-0652
info@journalofbabylon.com | jub@itnet.uobabylon.edu.iq | www.journalofbabylon.com

ISSN: 2312-8135 | Print ISSN: 1992-0652
info@journalofbabylon.com | jub@itnet.uobabylon.edu.iq | www.journalofbabylon.com

الخلاصة

المقدمة: لقد تمت دراسة التركيب النووي ل Ne^{20} بالتفصيل بأستخدام نموذج القشرة مع تقنيات باراميترات هارتزى – فوك لتوفير فهم أعمق لخصائصها التركيبية.

طرق العمل: استخدمت الدراسة فضاء نموذج psd مع التفاعل الفعال PSDMK ، مع الأخذ في الأعتبار He^4 هو قلب خامل. يتعامل النموذج مع الـ 16 نيوكليون المتبقية كجسيمات نشطة تتفاعل داخل الفضاء المحدد. تم الحصول على الدوال الموجية الشعاعية المطلوبة لحسابات عنصر المصفوفة بأستخدام طريقة هارتري – فوك مع جهود سكيرم مختلفة(SkXcsb, SkXta, and SLy4). بالإضافة إلى ذلك، تم استخدام الدوال الموجية للمذبذب التوافقي (HO)للتحليل المقارن لتقييم تأثير حالات الجسيمات الفردية المختلفة على الملاحظات النووية.

النتائج: تم تحليل العديد من الخصائص النووية بشكل منهجي، مثل عوامل شكل التشتت الإلكتروني الطولي، ومستويات الطاقة الأرضية، وشدة انتقال B (E2)، وعزم ثنائي القطب المغناطيسي، وعزم رباعي القطب الكهربائي، وجذر متوسط مربع نصف قطر الشحنة ، وطاقة الترابط الكلية.

الاستنتاجات: تُسلّط هذه الدراسة الضوء على أهمية استخدام قلب He^4 في حسابات نموذج القشرة لنواة Ne^{20}، وذلك من خلال نمذجتها كنظام من خمس عناقيد ألفا. وتشير النتائج إلى أن هذا النهج القائم على العناقيد يُحسّن التنبؤات النظرية، ويُقدّم إطارًا متينًا لاستكشاف ظواهر التركيب النووي في النوى الخفيفة.

الكلمات المفتاحية: نموذج القشرة، هارتزى فوك، التركيب النووي، فضاء نموذج psd ، قلب He^4 ، Ne^{20}.